Functional Materials 14, No.4 (2007)

Phase transformations at reduction of corundum

A.Ya.Dan'ko, M.A.Rom, N.S.Sidelnikova, Kh.Sh.Kaltaev, S.V.Nizhankovsky, A.I.Fedorov

Institute for Single Crystals, STC "Institute for Single Crystals", National Academy of Sciences of Ukraine, 60 Lenin Ave., 61001 Kharkiv, Ukraine

Received October 15, 2007

Research results are presented on the corundum structure transformation caused by reducing annealing. The annealing at 1500-2000°C in Ar atmosphere at $CO + H_2$ concentration 0.1-10 vol.% and N_2 0.1-0.4 vol.% has been found to result in the corundum transformation into aluminum oxynitride compounds with the spinel structure (γ-AlON) with the unit cell period of about 7.932 to 7.948 Å and wurtzite (AlN) with a≈3,107-3,115 and c≈4,979-4,988 Å. Possible mechanisms of the transformations are discussed.

Представлены результаты исследований трансформации структуры корунда в результате восстановительного отжига. Установлено, что отжиг при температуре 1500–2000°C в атмосфере Ar при концентрации $CO + H_2$ 0,1–10 об.% и N_2 — 0,1–0,4 об.% приводит к превращению корунда в оксинитридные соединения алюминия со структурой шпинели (γ-AlON) с периодом элементарной ячейки в пределах 7,932–7,948 Å и вюртцита (AlN) с a≈3,107–3,115 и c≈4,979–4,988 Å. Обсуждаются возможные механизмы наблюдаемых превращений.

When studying the formation of light scattering centers in sapphire crystals grown from a non-stoichiometric melt, the defects were supposed to be microscale inclusions of a phase having lower oxygen content than the corundum [1]. Later, the corundum transformation into spinel and a hexagonal symmetry phase during the reducing annealing was observed [2, 3]. This supposition was confirmed indirectly by the preparation conditions, the crystal-chemical transformation regularities, as well as by the mass gain in the obtained compounds under oxidation. However, the nature of stabilizers necessary to provide existence of those structures was not established unambiguously. When discussing the mechanism of the transformations observed, the vacancies formed due to the reduction were supposed to be capable of the valence reduction of the surrounding cations and thus act as a stabilizer. In this work, the further study results are presented for the peculiarities of phase transformations under high-temperature reduction of α-Al_2O_3, including the nature of the stabilizers for formed phases.

Plane-parallel sapphire samples and α-Al_2O_3 powders (15 to 25 μm particle size) with the main impurity content of ≤10 ppm were used in the studies. The reducing annealing was carried out in a furnace with carbon/graphite heat screens [4] at 1500 to 2000°C. The temperature was monitored by a Marathon MRISCSF integral IR pyrometer. The furnace was pre-heated up to 1500–1600°C under fore-vacuum pumping-out. After the residual pressure of about 0.1 to 0.3 Torr was attained, the furnace was filled with argon up to 800 Torr pressure. Due to the adsorbed oxygen and water vapor interaction with carbon/graphite materials, an atmosphere is spontaneously

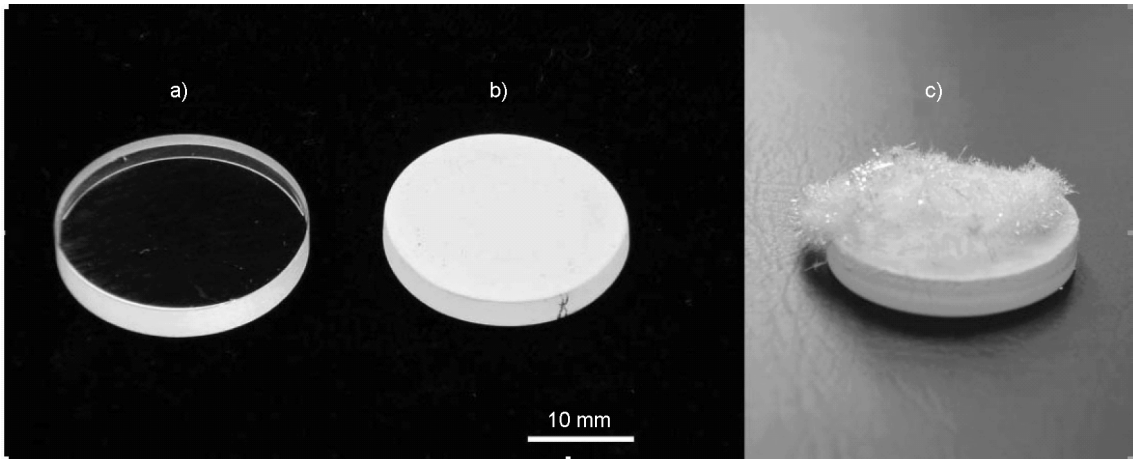

Fig. 1. Sapphire surface transformation due to reducing annealing: the initial polished sapphire sample (a); the sample with transformed about 30 μm thick near-surface layer (b); formation of needle-like crystals at the surface of transformed layer (c).

formed in the furnace containing mainly the reducing components, CO and H_2. The atmosphere composition was checked using a Kristall-200M gas chromatograph. The total concentration of the reducing components is about 0.1 to 0.5 %, the relative content of CO and H_2 varies within limits P_{H_2}/P_{CO} about 0.01 to 0.04, depending on the preliminary vacuum treatment. When necessary, the CO and H_2 concentration in the atmosphere was varied from 1 to 10 % (about 8 to 80 Torr) at various P_{H_2}/P_{CO} ratio values. In such cases, the following reducing additives were used: technical purity grade carbon dioxide that is a CO source due to carbon gasification reaction $C + CO_2 \rightarrow 2CO$; ethanol being a CO and H_2 source; chemical purity grade hydrogen prepared using a GV-6 hydrogen generator.

The main residual gas component in the annealing atmosphere is nitrogen, its concentration (C_{N_2}) after the standard vacuum pretreatment doing not exceed 0.4 vol. % (<1 Torr).

The reducing anneal of the single crystal samples results in transformation of a near-surface (up to 80 μm thick) sapphire layer into a polycrystalline one with a phase composition different from that of the bulk material (Fig. 1). The formation time of an up to 10 μm thick layer does not exceed 20 or 30 min. Similar changes of the phase composition are observed under reduction of α-Al_2O_3 powders. Typical diffraction patterns of the reduction products are presented in Fig. 2. According to X-ray phase analysis (XPA) results obtained using a DRON-1.5 diffractometer in Cu $K\alpha_{1,2}$ radiation (the (002) pyrographite monochromator) according to the θ–2θ scheme, the reduction products consist of two phases. One phase is cubic (space group Fd3m, a spinel), the other (H-phase), hexagonal (space group P63/mc, wurtzite structure). The lattice periods of the H-phase vary within the following limits: a, 3.107 to 3.115 Å; c, 4.979 to 4.988 Å; spinel, 7.932 to 7.948 Å, depending on the phase formation conditions. The annealing in the 1500 to 1700°C range results in corundum transformation into the H-phase. At higher temperatures, the phase composition varies from the phase mixture with a high (>98 %) H-phase content to essentially complete (within the XPA sensitivity limits) transformation into spinel.

When the single crystal samples are annealed, depending on the reduction conditions, dense transformed layers strongly bonded with the substrate are formed in some cases, while in other cases, the transformed layer has a loose structure and can be separated easily from the substrate. The dense H-phase and spinel layers show a more or less sharp texture along with an isotropic component. The studies of textured layers have shown that the new phases are formed under inheritance of the matrix crystallography, that is, the texture axis coincides with the normal to the corundum crystallographic plane and not with the normal to the sample geometric surface. In some cases, hexagonal needle-like crystals up to 0.1×5 mm^2 size have been observed to grow on the transformed layer surface (Fig. 1c). The crystals are characterized by a rather perfect although block structure (Fig. 3). Some crystals show bluish nuance as well as some areas of the transformed layer (Fig. 1c).

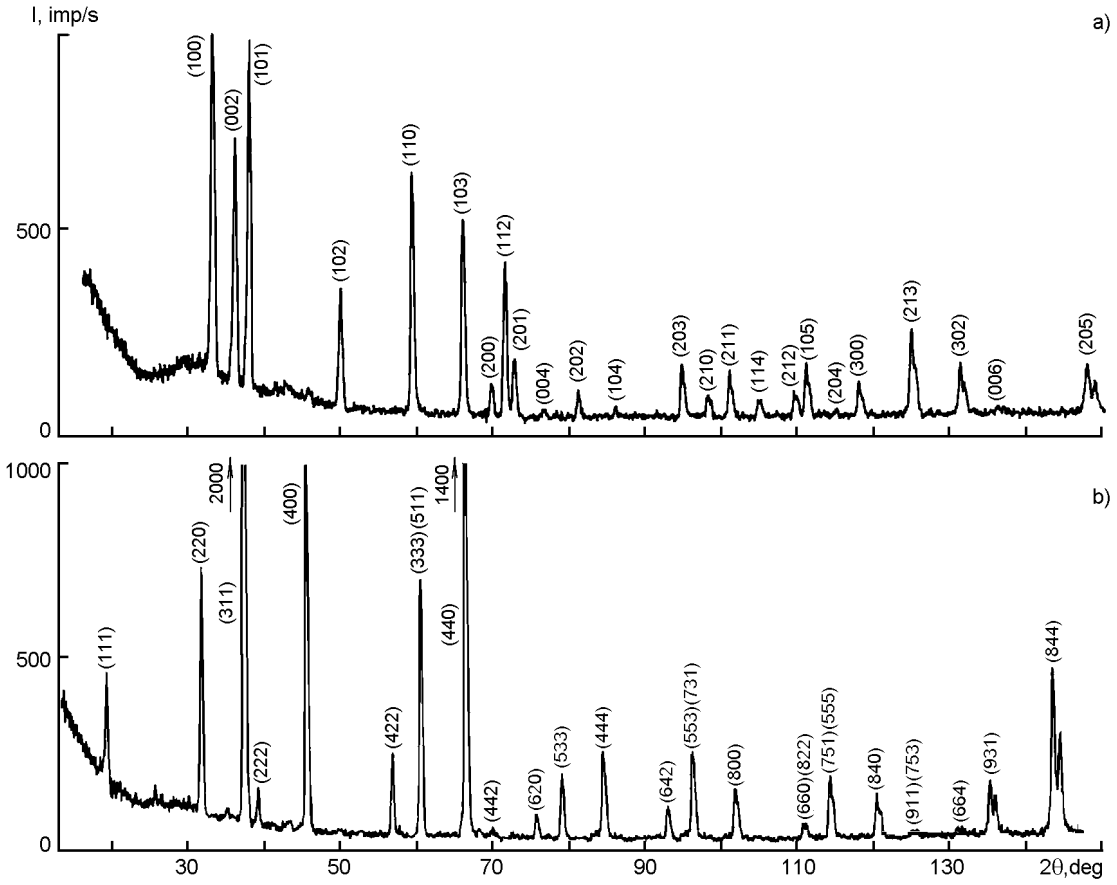

Fig. 2. X-ray diffraction patterns of corundum reduction products, Cu $K\alpha_{1,2}$ radiation: powder, H-phase >98 % (a = 3.111 Å; c = 4.979 Å) (a); powder, spinel >98 % (a = 7.941 Å) (b).

The formation conditions and structure characteristics of the phases mentioned are similar to those obtained in [5–8] where aluminum compounds in the Al–O system have been studied having a reduced (as compared to Al_2O_3) oxygen content. Although the data on those compounds are scarce, the physical, optical, chemical and some other characteristics have been determined [5–7], and thermodynamic properties of the spinel phase have been estimated [9]. The formation mechanism of oxygen-depleted phases assumes that under reduction, a supersaturated solution of anionic vacancies is formed in the oxide lattice that is then decomposed under isolation of nuclei of phases being equilibrium under the specified conditions [8]. At the same time, the structure characteristics of compounds obtained by us are rather similar to those of well-known phases with spinel and wurtzite structures in the Al_2O_3–Al_4C_3 and Al_2O_3–AlN systems [10–14]. It is to note that the earlier thermodynamic estimations [15] did not

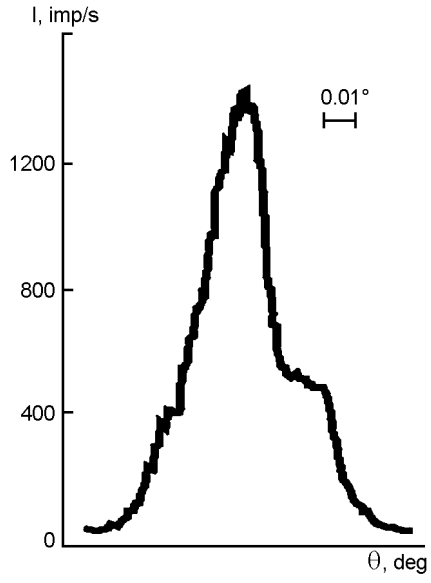

Fig. 3. X-ray rocking curve from a colorless needle-like crystal. DRON-3 diffractometer, (n, $-m$) scheme, {101} reflection, Cu $K\alpha_1$ radiation (monochromator Ge (111)).

Table 1. Impurity content in the corundum reduction products

No.	Preparation conditions	Phase composition (XPA data)	Impurity concentration, wt. %		
			N	C	H
1	1900°C, Ar (≈0.5 % CO)	Spinel >98 %	3.7–4.5	0.08–0.09	0.1–0.17
2	1800°C, Ar(≈7 % CO)	Spinel ≈92 %, H-phase ≈5 %, corundum ≈3 %	5.77	0.25	0.18
3	1795°C, Ar(≈2 % CO)	Spinel ≈85 %, H-phase ≈10 %, corundum ≈5 %	8.07	0.44	0.13
4	1950°C, Ar (≈0.2 % CO)	H-phase >98 % (white powder)	≈25.37	0.32–0.57	0.1–0.4
5	1950°C, Ar (≈0.2 % CO)	H-phase >98 % (bluish powder)	23.2–24.1	0.8–0.75	0.17–0.27
6	1950°C, Ar(≈0.2 % CO)	Needle-like crystals (colorless)	26.9	0.4	–
7	1950 °C, Ar (≈0.2 % CO)	Needle-like crystals (bluish)	27.4	0.7	–

forecast the formation possibility of oxycarbides in appreciable amounts under the experimental conditions. The formation possibility of oxynitride compounds was not considered at first due to low nitrogen concentrations in the annealing atmosphere [2, 3].

The powders obtained in various conditions and the needle-shaped crystals were analyzed chemically using an EUROEA-3000 elemental analyzer (see Table 1). The analysis results show that the nitrogen concentration in the samples attains rather high values while carbon is present at concentrations lower than 1 % and is not a primary impurity. The transformed surface layers of the single crystal samples containing up to 98 % of the H-phase comprise also an increased nitrogen amount, as is shown using a Kratos XPS-800 X-ray photoelectron spectrometer. Thus, it follows from the chemical analysis data that the phases obtained are compounds of the Al_2O_3–AlN system. Two groups of aluminum oxynitride phases are known within that system, one based on the AlN wurtzite structure (AlN>50 mol. %) and the other, on the Al_2O_3 structure (AlN<50 mol.%). The most widespread model of the aluminum oxynitride (AlON) structure, including the spinel phase (γ-AlON), is the model containing a constant number of anions [14, 16]. Within that model, the structure formula of the compound can be presented as

$$Al_{(64+x)/3}V^{C}_{(8-x)/3}O_{(32-x)}N_x , \qquad (1)$$

where V^C are cationic vacancies the presence of which is conditioned by the preservation of electric neutrality. Proceeding from those concepts, the spinel phase obtained by us (No.1 in Table 1) has the composition $(AlN)_{0.23}\cdot(Al_2O_3)_{0.77}$ – $(AlN)_{0.27}\cdot(Al_2O_3)_{0.73}$ (or about $AlN\cdot 3Al_2O_3$) that is within the spinel phase stability region in the phase diagram of Al_2O_3–AlN system [11]. As the H-phase content rises, the nitrogen concentration in the samples increases (Nos. 2, 3 in Table 1) and attains about 23 to 25 % for the H-phase (Nos. 4, 5) approaching to that in AlN (about 34 %). Basing on the nitrogen concentration data, the H-phase samples have the composition $(AlN)_{0.84}\cdot(Al_2O_3)_{0.16}$ – $(AlN)_{0.88}\cdot(Al_2O_3)_{0.12}$ or $\approx 5(AlN)\cdot(Al_2O_3)$ – $7(AlN)\cdot(Al_2O_3)$ and coincide to the 21R and 27R polytypes in the phase diagram [11].

Possible models were considered for the crystal structure of compounds obtained. When calculating the model X-ray diffraction pattern (using the POWDER CELL v.2.3 software [17]), the experimental values of lattice periods and the chemical analysis data (Table 1) were used to determine the occupancy of the symmetry positions. The temperature factor was not taken into account ($B = 0$). When constructing the models, the calculated and experimental diffraction pattern were compared for all the diffraction lines within the 2θ range from 10° to 150°. The R-factor value $R = \sum|I_{exp} - I_i^{exp}|/\ \sum I_i^{calc}$ was used as the model validity criterion, where I_i^{exp} and I_i^{calc} are the experimental and calculated relative intensity of the i-th reflection, respectively. When simulating the spinel structure, a good agreement with the experimental results was obtained for the model similar to γ-AlON (Table 2). When comparing the calculated data with the experimental diffraction pattern (Fig. 2b) for

Table 2. Atomic coordinates in model structure of spinel crystal (Fd3m, a = 7.941 Å)

Atom	Position	Coordinate			Occupancy
		x	y	z	
Al	8a	0	0	0	1
Al	16d	0.625	0.625	0.625	0.895–0.91
O	32e	0.38	0.38	0.38	0.908–0.887
N	32e	0.38	0.38	0.38	0.092–0.113

Table 3. Atomic coordinates in model structure of H-phase crystal (P63/mc, wurtzite structure, a = 3.111 Å; c = 4.979 Å)

Atom	Position	Coordinate			Occupancy
		x	y	z	
Al	2b	0.3333	0.6667	0	0.9
O	2b	0.3333	0.6667	0.383	0.29
N	2b	0.3333	0.6667	0.383	0.71

the compound No.1 (Table 1), the R-factor calculated on the basis of all the 22 observed interference lines amounts about 0.12, while being about 0.072 if the lines within the 110° to 150° range (where the temperature factor is more pronounced) are neglected. Thus, the model provides an adequate description of the compound obtained in experiment.

The structure of H-phase was described using a model similar to AlN (Table 3). When comparing the calculated data with the experimental diffraction pattern (Fig. 2a) of the compound No.4 (Table 1) to that the composition $Al_{0.9}O_{0.29}N_{0.71}$ is ascribed basing on the model with constant number of anions ($Al_{1-x/3}O_xN_{1-x}$ [18]), the R-factor calculated on the basis of all the 24 observed interference lines amounts about 0.075, while being about 0.072 if the lines within the 110° to 150° range are neglected. Thus, the H-phase is of AlN structure, although at such nitrogen concentrations, the 27R ($Al_9O_3N_7$) and 21R ($Al_7O_3N_5$) are observed according to literature data [11].

The needle-shaped crystals consist of aluminum oxynitride compounds, too. The composition thereof (Nos. 6 and 7, Table 2) is close to $7AlN{\cdot}Al_2O_3$ or $8AlN{\cdot}Al_2O_3$ polytypes [19] and the growth seems to occur from the gas phase, perhaps due to Al and Al suboxides interation with N_2 as is supposed in [19]. The nitrogen concentration decrease in the atmosphere down to <0.1 vol. % does not affect in principle the corundum transformation character but no needle-like crystals are formed in this case. The bluish color of some needle-like crystals as well as some areas in the transformed layer may be connected with the carbon impurity having an increased concentration in those samples (Table 1).

The formation conditions of various compounds in the Al_2O_3–AlN system are under rather intensive studies, however, no literature data are available on the AlN and γ-AlON formation in similar conditions. The aluminum nitride and oxynitride are synthesized as a rule in nitrogen or nitrogen-containing gases (NH_3–C_3H_8, NH_3–H_2 and other mixtures). At carbon-thermal reduction of AlN and AlON, mixtures of various polymorphs of aluminum oxide (γ, δ, θ, α) with carbon are obtained in nitrogen [21, 22] or air [13] atmosphere. There are few studies on AlN and AlON formation at the corundum surface under heating in CO–N_2 mixtures, the mixture with a high nitrogen concentration ($P_{CO}/P_{N2}\approx0.1$) being used in those works [22]. When discussing the AlN and AlON formation mechanism, the following reactions are considered in those cases [23, 24]:

$$Al_2O_3(s) + 3C(s) + N_2(g) = 2AlN(s) + 3CO(g), \quad (2)$$

$$[(64 + x)/3x]Al_2O_3(s) + 3C(s) + N_2(g) = (2/x)Al_{(64+x)/3}O_{32-x}N_x + 3CO(g). \quad (3)$$

In our experiments, corundum does not contact directly with carbon, thus, the observed phase transformations could be supposed to occur under involvement of reducing gases CO and H_2:

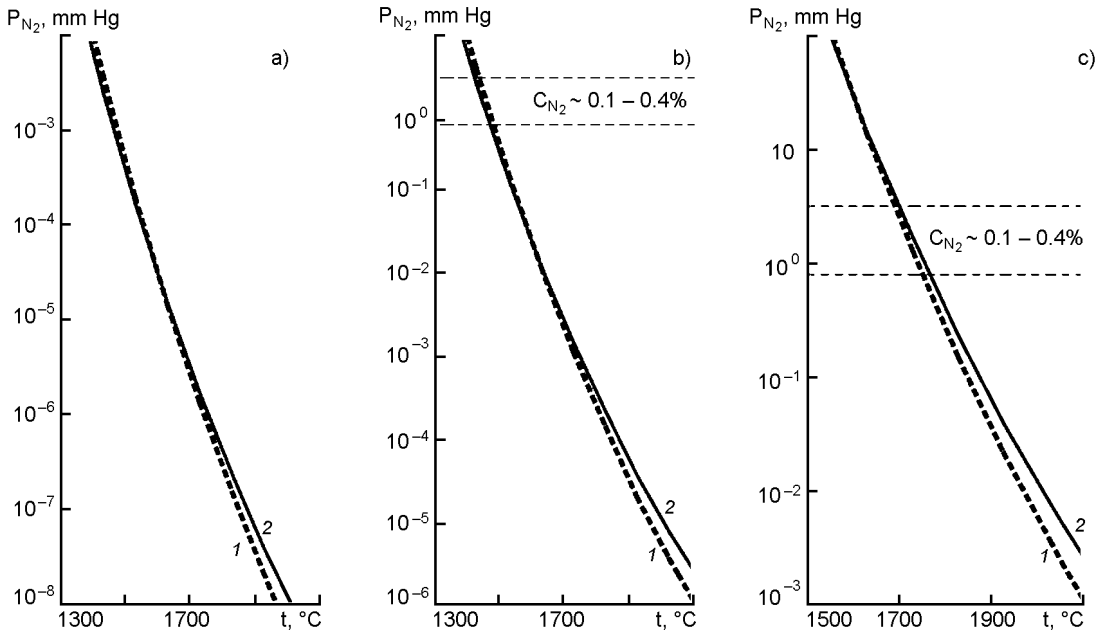

Fig. 4. P_{N_2} estimations at CO concentration in the annealing atmosphere (vol. %): 0.1 (a); 1 (b); 10 (c). Curves *1* for reaction (4); curves *2* for reaction (8).

$$Al_2O_3(s) + 3CO(g) + N_2(g) = 2AlN(s) + 3CO_2(g), \quad (4)$$

$$[(64 + x)/3x] \cdot Al_2O_3(s) + 3CO(g) + N_2(g) = (2/x) \cdot Al_{(64+x)/3}O_{32-x}N_x(s) + 3CO_2(g), \quad (5)$$

$$Al_2O_3(s) + 3H_2(g) + N_2(g) = 2AlN(s) + 3H_20(g), \quad (6)$$

$$[(64 + x)/3x]Al_2O_3(s) + 3H_2(g) + N_2(g) = (2/x)Al_{(64+x)/3}O_{32-x}N_x(s) + 3H_2O(g). \quad (7)$$

The AlN and AlON formation probability for the case of reduction with CO as the main reducing component of the gas phase was estimated thermodynamically. Fig. 4 presents the estimated equilibrium pressure of nitrogen (P_{N_2}) for reaction (4) and formation of γ-AlON ($AlN{\cdot}3Al_2O_3$, No.1, Table 1) according to the reaction

$$7Al_2O_3 + 3CO + N_2 = 2[AlN \cdot 3Al_2O_3] + 3CO_2\uparrow, \quad (8)$$

within the experimental CO concentration range of 0.1 to 10 vol. %. In the calculations, the formation energy values for AlN: $\Delta G^o(AlN) = -316.2 + 0.1157T$ [23] and for $AlN{\cdot}3Al_2O_3$: $\Delta_f G^o(Al_7O_9N) = -5315.2132 + 1.054520T$ [25] were used as well as the reference data [26] and the assumption that the ratio P_{CO_2}/P_{CO} is defined by the equilibrium of the reaction $C + CO_2 = 2CO$. It follows from the estimations that at the CO concentration in the atmosphere about 1 vol. %, the reactions (4) and (8) are possible at temperatures exceeding 1500°C even if P_{N_2} values are lower than those observed in experiment (Fig. 4a). At a lower CO concentration, the P_{N_2} is still lower (Fig. 4a). As the CO pressure increases, higher C_{N_2} are necessary to generate the phases mentioned, however, C_{N_2} does not exceed 0.4 vol. % at $T >$ 1700°C (Fig. 4c).

In contrast to AlN and AlON formation under carbon-thermal reduction where the reactions (2) and (3) occur in the whole bulk of the Al_2O_3/carbon reaction mixture, the reactions (4), (5) and (8) result in phase transformations only at the surface contacting directly with the gas atmosphere. The formation of transformed layer with a thickness attaining about 80 μm in some cases suggests the penetration of the oxynitride layer formed at the surface deep into the crystal, the penetration mechanism being unclear. A mechanism including reduction and diffusion seems to be rather probable; that mechanism has been supposed

basing on the results obtained at the spinel phase oxidation.

Basing on (1), the spinel phase obtained by us and containing 3.7 to 4.5 wt. % of nitrogen corresponds to a structure formula similar to $AlN{\cdot}3Al_2O_3$. When the compound is oxidized according to the reaction

$$2(AlN \cdot 3Al_2O_3) + 3/2O_2 \rightarrow 7Al_2O_3 + N_2\uparrow,$$

the mass must increase by about 3 %. However, a mass gain of 5.6 to 6 % was observed in oxidation experiments on the spinel phase powder. Such a considerable discrepancy cannot be ascribed to the presence of carbon (about 0.1 wt. %) in the compound (Table 1). It is to note that oxidation of spinel phase obtained by sintering of AlN and Al_2O_3 [27] results in the mass gain corresponding to nitrogen content in the compound. At the same time, when oxidizing the spinel phase obtained by carbonthermal reduction, the mass gain about 6.9 % was observed [13], thus, the compound obtained could be assumed to be the stoichiometric oxynitride spinel $AlN{\cdot}Al_2O_3$. However, such a composition was shown later [11, 14, 16] to be outside of the spinel phase stability region in the $AlN–Al_2O_3$ system. One of possible reasons for that discrepancy may consist in that the true composition of the reduced spinel phase differs from that calculated using (1). According to direct estimations, the experimental mass gain of 5.6 to 6 % coincides with the calculated one for the composition $Al_{2.98}O_{3.6}N_{0.4}$, i.e., when the number of occupied cationic positions exceeds that calculated using (1) ($Al_{2.8}O_{3.6}N_{0.4}$). If that structure formula is presented formally as $AlN{\cdot}3(Al_2O_{2.8}V^A_{0.2})$ (where V^A denotes anionic vacancy), then the compounds obtained can be considered as phases in the $AlN–Al_2O_{3-x}V^A_x$ system.

Summarizing the data obtained, the presence of a high concentration of anionic vacancies in corundum can be supposed to favor the nitrogen diffusion into the matrix and the phenomena observed to result from reactions of dissolved nitrogen with anion-defected corundum. The formation probability of oxynitride compounds is defined in this case, in particular, by surface reactions (4) and (5). Perhaps one step of the crystal-chemical transformation may consist in formation of oxygen-deficient metastable phases in the $Al–Al_2O_3$ system that are stabilized in part with nitrogen. In that case, the anionic vacancies in corundum may contribute to conservation of electric neutrality in the compounds obtained. However, at present, there is no unique description of crystal-chemical reactions resulting in oxynitride phases formation in a macroscale near-surface volume of a crystal under reducing annealing in atmosphere with low nitrogen concentration.

The results obtained are of a considerable interest in connection with ever-widening application field of materials belonging to the $AlN–Al_2O_3$ system, including nitride and oxynitride layers at sapphire surfaces [22]. The results give also rise to assumption that the light scattering centers in sapphire crystals grown from non-stoichiometric melt [1] may occur under involvement of nitrogen.

References

1. A.Ya.Dan'ko, N.S.Sidel'nikova, G.T.Adonkin et al., *Crystallography Report*, **49**, 240 (2004).
2. A.Ya.Dan'ko, M.A.Rom, N.S.Sidelnikova et al., *Functional Materials*, **12**, 725 (2005).
3. A.Ya.Dan'ko, M.A.Rom, N.S.Sidelnikova et al., *Poverkhnost: Roentgen., Synkhrotron. and Neutron Issled.*, **11**, 89 (2005).
4. A.Ya.Dan'ko, N.S.Sidelnikova, G.T.Adonkin et al., *Functional Materials*, **4**, 92 (1997).
5. M.S.Beletsky, M.B.Rapoport, *Dokl.AN SSSR*, **80**, 751 (1951).
6. N.E.Filonenko, I.V.Lavrov, S.V.Andreeva et al., *Dokl.AN SSSR*, **115**, 583 (1957).
7. Zh.L.Vert, M.V.Kamantsev, V.I.Kudryavtsev et al., *Dokl.AN SSSR*, **116**, 834 (1957).
8. A.V.Roshchin, V.E.Roshchin, *Metally*, **1**, 3 (2006).
9. A.V.Aponchuk, O.M.Katkov, I.K.Karpov, *Izv VUZov: Tsvetnaya Metallurgia*, **6**, 50 (1986).
10. Yu.I.Ryabkov, V.E.Grass, P.A.Sitnikov, *Zh. Obshch. Khim.*, **72**, 181 (2002).
11. C.Qiu, R.Metselaar, *J.Am.Ceram.Soc.*, **80**, 2013 (1997).
12. G.Long, L.M.Foster, *J.Am.Ceram.Soc.*, **44**, 255 (1961).
13. G.Yamaguchi, H.Yanagira, *Chem.Soc.Japan Bull.*, **32**, 1264 (1959).
14. Chang Ming Fang, R.Metselaar, H.T.Hintzen, G.de With, *J.Am.Ceram.Soc.*, **84**, 2633 (2001).
15. A.Ya.Dan'ko, N.S.Sidelnikova, V.N.Kanischev et al., *Functional Materials*, **5**, 243 (1998).
16. W.J.McCauley, *J.Am.Ceram, Soc.*, **61**, 372 (1978).
17. W.Kraus, G.Nolze, *J.Appl.Crystallogr.*, **29**, 301 (1996).
18. J.Rosa, I.Tale, *Czech.J.Phys.*, **B29**, 818 (1979).
19. G.J.Jiang, H.R.Zhuang, W.L.Li et al., *J.Mat. Synth. and Proc.*, **7**, 1 (1999).

20. W.Rafaniello, I.B.Cutler, *Com. Am. Ceram. Soc.*, , 128 (1981).
21. T.S.Bartnitskaya, N.F.Ostrovskaya, G.N.Makarenko et al., *Powder Metallurgy and Metal Ceramics*, **41**, 232 (2002).
22. H.Fukuyama, S.Kusunoki, A.Hakomoriet et al., *J. Appl. Phys.*, **100**, 024905-1 (2006).
23. W.Nakao, H.Fukuyama, K.Nagata, *J. Am. Ceram. Soc.*, **85**, 889 (2002).
24. L.Yawei, L.Nan, Y.Runzhang, *J. Mat. Science*, **34**, 2547 (1999).
25. X.Wang, W.Li, S.Seetharaman, *Scandinavian J. Metallurgy*, **31**, 1 (2002).
26. Thermodynamic Properties of Individual Substances, vol.2, ed. by V.P.Glushko, AN SSSR Publ., Moscow (1962) [in Russian].
27. X.Wang, D.Sichen, W.Li et al., *Met. and Mat. Trans.*, **33B**, 201 (2002).

Фазові перетворення при відновленні корунду

О.Я.Данько, М.А.Ром, Н.С.Сідельнікова, Х.Ш-о.Калтаєв, С.В.Ніжанковський, О.І.Федоров

Представлено результати досліджень трансформації структури корунду в результаті відновного відпалу. Установлено, що відпал при температурі 1500–2000°С в атмосфері Ar при концентрації CO + H_2 0,1–10 об. % та N_2 — 0,1–0,4 об. % приводить до перетворення корунду в оксинітридні сполуки алюмінію зі структурою шпінелі (γ-AlON) з періодом елементарної гратки у межах 7,932–7,948 Å і вюртціту (AlN) з a≈3,107–3,115 та c≈4,979–4,988 Å. Обговорюються можливі механізми перетворень, що спостерігалися.